Ag Alloying and KF Treatment Effects on Low Bandgap CIGS Solar Cells

Nicholas Valdes¹, JinWoo Lee², William Shafarman¹

¹ University of Delaware and Institute of Energy Conversion, Newark, DE

² Global Solar Energy Inc., Tucson, AZ

Abstract — Silver alloying and KF post-deposition treatments are 2 approaches to increase the efficiency of CIGS solar cells. Although it has been shown in the literature that KF improves ACIGS device performance for reduced KF amounts, in present studies of lower bandgap ACIGS, KF is detrimental on $V_{\rm OC}$. J-V curves also exhibit light-to-dark crossover in ACIS+KF films. This has motivated a study on the growth of CdS on low bandgap (A)CIS films with and without KF. SEM and GDOES suggest a different CdS growth on Ag alloyed CIS.

Index Terms — Ag alloying, Cu(In,Ga)Se₂ (CIGS) solar cells, potassium fluoride post-deposition treatment (KF-PDT).

I. INTRODUCTION

Silver alloyed CIGS (ACIGS) solar cells have beneficial properties such as larger grain sizes, improved lifetime, and enhanced current collection [1]. Ag alloys also have a lower melting temperature which hypothetically allows for a reduced processing temperature. The efficiency of ACIGS solar cells can be improved with a KF post-deposition treatment (PDT) but only with a significantly less amount of KF compared to CIGS [2]. However, those results were obtained in ACIGS with Ga/(Ga+In) \approx 0.4. The combined effect of Ag alloying and KF-PDT has not been studied for lower bandgap $E_{\rm g} < 1.1$ eV CIGS which has relevance for bottom cells in tandems.

In this work, Ag alloyed CIS (ACIS, no Ga) is shown to have considerable performance losses with the KF-PDT regardless of the KF thickness with the main loss in $V_{\rm OC}$. It is shown that the CdS growth is different with Ag alloying and KF, which can affect the device behavior.

II. EXPERIMENTAL DETAILS

CIS and Ag alloyed CIS (ACIS) were deposited by three-stage co-evaporation with a substrate temperature of 580° C. After the chalcopyrite deposition, the substrates were cooled to 350° C and held at that temperature for 7.5 min. At this point, standard absorber layers received only Se flux, but KF treated samples received both KF and Se flux. The target KF thickness was 7.5 nm. The resulting absorber layer compositions were (Ag+Cu)/In \approx 0.85 and Ag/(Ag+Cu) \approx 0.1-0.2 with thicknesses between 1.8-2.3 μ m as determined by x-ray fluorescence. Bandgap (E_g) values were determined by spectrophotometry and the long wavelength edge of quantum efficiency (QE) measurements.

Samples that were made into devices had the following device structure: SLG/Mo/(A)CIS/CdS/i-ZnO/ITO/Ni+Al grids. CdS was deposited by chemical bath deposition. All samples were rinsed in a DI water bath before the CdS deposition. Samples for devices were pulled out of the CdS bath after 11.5 min. ("thin") or 14 min. ("regular"). The corresponding CdS thicknesses are about 35 and 50 nm respectively. Samples for scanning electron microscope (SEM) imaging were pulled out of the bath after 6.5 min. corresponding to ~ 10 nm thickness.

Current-voltage (*J-V*) measurements were performed at 25°C with AM1.5 illumination. SEM images were taken with a JEOL JSM-7400F at 3 kV. Compositional depth profiling was performed using Glow Discharge Optical Emission Spectroscopy (GDOES).

III. RESULTS AND DISCUSSION

A. Comparison of Device Performance With and Without Ag Alloying

Table I compares the performance of the best CIS and ACIS devices in this work. Under these growth conditions, there is

 $\label{eq:Table I} \mbox{Device performance of best cells of CIS and ACIS} \\ \mbox{In this study}$

Sample	$E_{\rm g}$ (eV)	V _{OC} (mV)	$J_{\rm SC}$ (mA/cm ²)	FF (%)	η (%)
CIS	1.00	472	37.1	71.5	12.5
ACIS	1.02	455	36.6	71.8	12.0

no significant change in efficiency when alloying with Ag. There is usually a decrease in the $V_{\rm OC}$ with Ag addition despite the increase in bandgap. This decrease is likely due to the reduced carrier concentration with Ag incorporation, which was determined by capacitance-voltage measurements (not shown here). Although $J_{\rm SC}$ for the best ACIS is less than CIS in Table II, generally an increase in $J_{\rm SC}$ is observed in ACIS. This in turn corresponds to an increased current collection in the long wavelength QE (not shown).

B. Effect of KF Treatment and Buffer Layer Thickness on Device Performance

Table II compares $V_{\rm OC}$ of the best devices of each condition (with and without Ag, with and without KF) having either a

Table II Highest $V_{\rm OC}$ values for regular (~ 50 nm) and thin (~ 35 nm) CdS buffer layers, along with the difference between the two $V_{\rm OC}$ values

Sample	Regular CdS $V_{\rm OC}$ (mV)	Thin CdS $V_{\rm OC}$ (mV)	$\Delta V_{ m OC}$ (Reg. – Thin) (mV)
CIS	474	464	- 10
CIS+KF	485	487	+ 2
ACIS	469	460	- 9
ACIS+KF	411	436	+ 25

regular (~ 50 nm) or thin (~ 35 nm) buffer layer. The KF treatment improves the $V_{\rm OC}$ of CIS solar cells as anticipated. There is a slight decrease in $V_{\rm OC}$ when CIS is alloyed with Ag, and a larger decrease in $V_{\rm OC}$ when ACIS is exposed to a KF treatment. Further, most ACIS+KF samples in this work have $V_{\rm OC}$ values less than 400 mV. Although the results are shown for 7.5 nm KF, the drop in $V_{\rm OC}$ for the ACIS+KF film occurred for thicknesses between 0.5-3 nm as well. It also occurred for small amounts of Ga alloying (GGI ≈ 0.05).

With respect to CdS thickness, the $V_{\rm OC}$ of both CIS and ACIS decreases when the buffer layer thickness is reduced, likely due to incomplete surface coverage (indicated by a negative $\Delta V_{\rm OC}$ value). In the CIS+KF samples, the $V_{\rm OC}$ does not change with the decreased buffer thickness. However, for ACIS+KF the $V_{\rm OC}$ increases when the CdS buffer layer is reduced.

A comparison of light and dark J-V behavior yields additional insight into these $V_{\rm OC}$ effects. Fig. 1 shows the light and dark J-V curves of representative ACIS and ACIS+KF devices. ACIS solar cells display superposition of the light

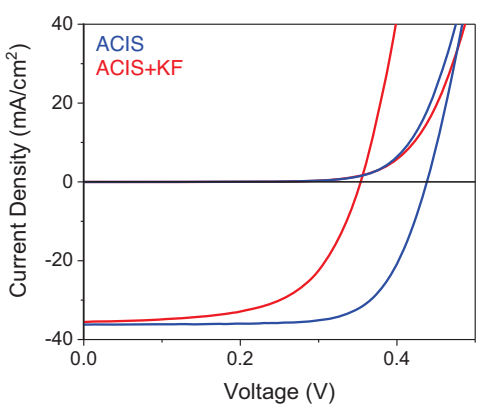


Fig. 1. *J-V* curves for representative ACIS (blue) and ACIS+KF (red) solar cells, both with the regular CdS thickness.

and dark curves, however, ACIS+KF have light-to-dark crossover. This behavior is normally attributed to photoconductivity in the CdS layer [3]. Some CIS+KF devices in this study also show light-to-dark crossover, but not to the same extent as ACIS+KF. Because CIS+KF solar cells are

known to have faster CdS nucleation than CIS and some CIS+KF have light-to-dark crossover, the $V_{\rm OC}$ loss in ACIS+KF could be related to its CdS growth. Edoff et al. claimed that some of their ACIGS films with the KF treatment demonstrated forward bias rollover which could indicate a conduction band barrier [2], but this has not been observed in our samples under standard testing conditions.

C. Initial Characterization of CdS Growth and Distribution

Because the *J-V* results suggest a detrimental influence from CdS on the device performance of ACIS+KF, SEM was performed to investigate the CdS growth on each absorber. Fig. 2 shows SEM images of the 4 sample types of this study, each after 6.5 min of CdS deposition. The samples were

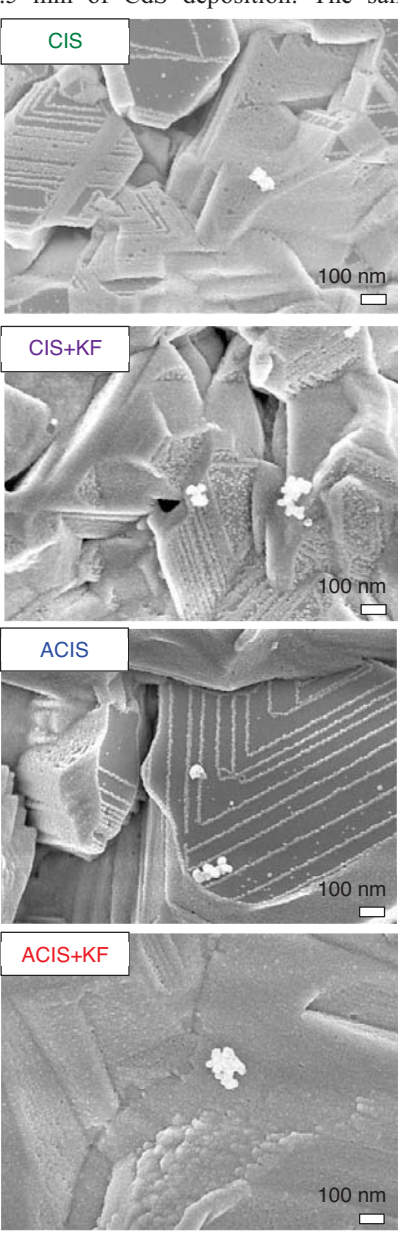


Fig. 2. SEM images from top to bottom: CIS, CIS+KF, ACIS, and ACIS+KF after 6.5 min. CdS deposition time.

placed in the same CdS bath to eliminate bath-to-bath variability. Dark areas correspond to an uncovered absorber layer and brighter areas correspond to CdS [4]. The CIS film shows some grains with slower CdS growth, likely attributed to (112) planes [4]. The CIS+KF sample is not completely covered at 6.5 min., but there is improved coverage of CdS compared to CIS. ACIS shows some grains that are fully covered and large area grains that are not covered. It is speculated that the grains that are not fully covered and are forming triangular patterns are (112) similar to CIS [4], [5], but electron backscatter diffraction (EBSD) would be needed to verify this. The ACIS+KF sample however, shows complete coverage even at 6.5 min. All SEM observations were seen in multiple areas of the films. Furthermore, an initial x-ray photoelectron spectroscopy (XPS) study of a similar sample set suggested that ACIS+KF had the highest concentration of Cd and S on the surface of the film (not shown here).

To verify if these effects were limited to the surface, GDOES was performed on complete devices with a thin CdS buffer to obtain the compositional distribution of the CdS buffer layer. Fig. 3 shows the Cd distribution of each sample type in this study. The Cd in CIS+KF appears to be distributed

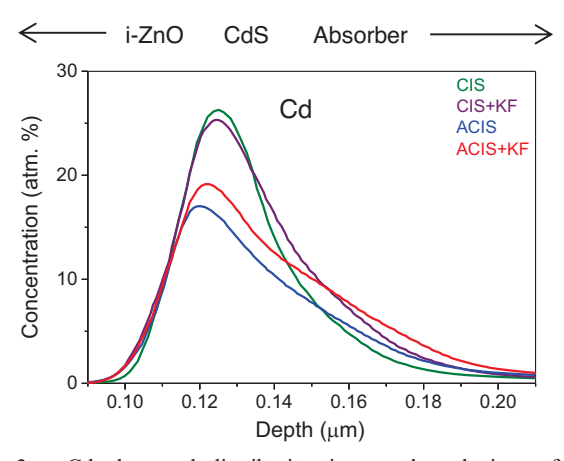


Fig. 3. Cd elemental distribution in complete devices of the 4 different absorber layers, each with thin CdS layers.

deeper into the absorber compared to CIS, as would be anticipated from the increased Cd incorporation in KF treated films. For Ag alloys however, the distribution is different. The concentration of Cd at the i-ZnO/CdS interface is less than the non-Ag samples, and appears to penetrate more deeply into the absorber. Although not shown, the distribution of S is similar to Cd.

IV. CONCLUSIONS

The effects of Ag alloying and KF treatments on CIS-based solar cells were presented. The addition of Ag did not have a significant effect on the device performance of CIS-based devices. KF treatments improved CIS, but had a detrimental impact on the $V_{\rm OC}$ of ACIS. Light-to-dark crossover was seen in ACIS+KF, which is related to CdS defects. Both SEM and GDOES indicated different growth of CdS with KF and Ag alloying. Additional device characterization and diode analysis will be done to correlate changes in carrier concentration and activation energy of recombination with $V_{\rm OC}$ of these devices and changes in the CdS properties.

ACKNOWLEDGEMENTS

This project was funded by the National Science Foundation under award number 1507291.

REFERENCES

- [1] R. L. Garris, S. Johnston, J. V. Li, H. L. Guthrey, K. Ramanathan, and L. M. Mansfield, "Electrical characterization and comparison of CIGS solar cells made with different structures and fabrication techniques," Sol. Energy Mater. Sol. Cells, vol. 174, no. August 2017, pp. 77–83, 2018.
- [2] M. Edoff, T. Jarmar, N. S. Nilsson, E. Wallin, D. Högström, O. Stolt, O. Lundberg, W. Shafarman, and L. Stolt, "High Voc in (Cu,Ag)(In,Ga)Se₂ solar cells," *IEEE J. Photovoltaics*, vol. 7, no. 6, pp. 1789–1794, 2017.
- [3] A. Kylner, "Effect of impurities in the CdS buffer layer on the performance of the Cu(In,Ga)Se₂ thin film solar cell," *J. Appl. Phys.*, vol. 85, no. 9, p. 6858, 1999.
- [4] W. Witte, D. Abou-Ras, and D. Hariskos, "Chemical bath deposition of Zn(O,S) and CdS buffers: Influence of Cu(In,Ga)Se₂ grain orientation," *Appl. Phys. Lett.*, vol. 102, no. 5, 2013.
- [5] D. Liao and A. Rockett, "The structure and morphology of (112)-oriented Cu(In,Ga)Se₂ Epitaxial Films," *J. Appl. Phys.*, vol. 104, no. 2009, p. 8, 2008.